Development and evaluation of a CEACAM6-targeting theranostic nanomedicine for photoacoustic-based diagnosis and chemotherapy of metastatic cancer

Hohyeon Lee [a], Yongho Jang [a], Suhyun Park [a], Hyejin Jang [a], Eun-Joo Park [b], Hyun Jung Kim [c] and Hyuncheol Kim [a,d]

[a] Department of Chemical & Biomolecular Engineering, Sogang University, #1 Shinsu-dong, Mapo-gu, Seoul, 121-742, Republic of Korea

[b] Biomedical Research Institute & Department of Radiology, Seoul National University Hospital, 101 Daehak-ro, Jongno-gu, Seoul, 03080, Republic of Korea

[c] Department of Biomedical Engineering, The University of Texas at Austin, Austin, TX 78712, USA

[d] Department of Biomedical Engineering, Sogang University, #1 Shinsu-dong, Mapo-gu, Seoul, 121-742, Republic of Korea

Corresponding author: Hyuncheol Kim, Ph.D.

Department of Chemical & Biomolecular Engineering, Department of Biomedical Engineering, Sogang University, #35 Baekbeom-ro, Mapo-gu, Seoul 121-742, Republic of Korea

Tel: +82-2-705-8922, Fax: +82-2-3273-0331, E-mail: hyuncheol@sogang.ac.kr

Supplementary Figure S1

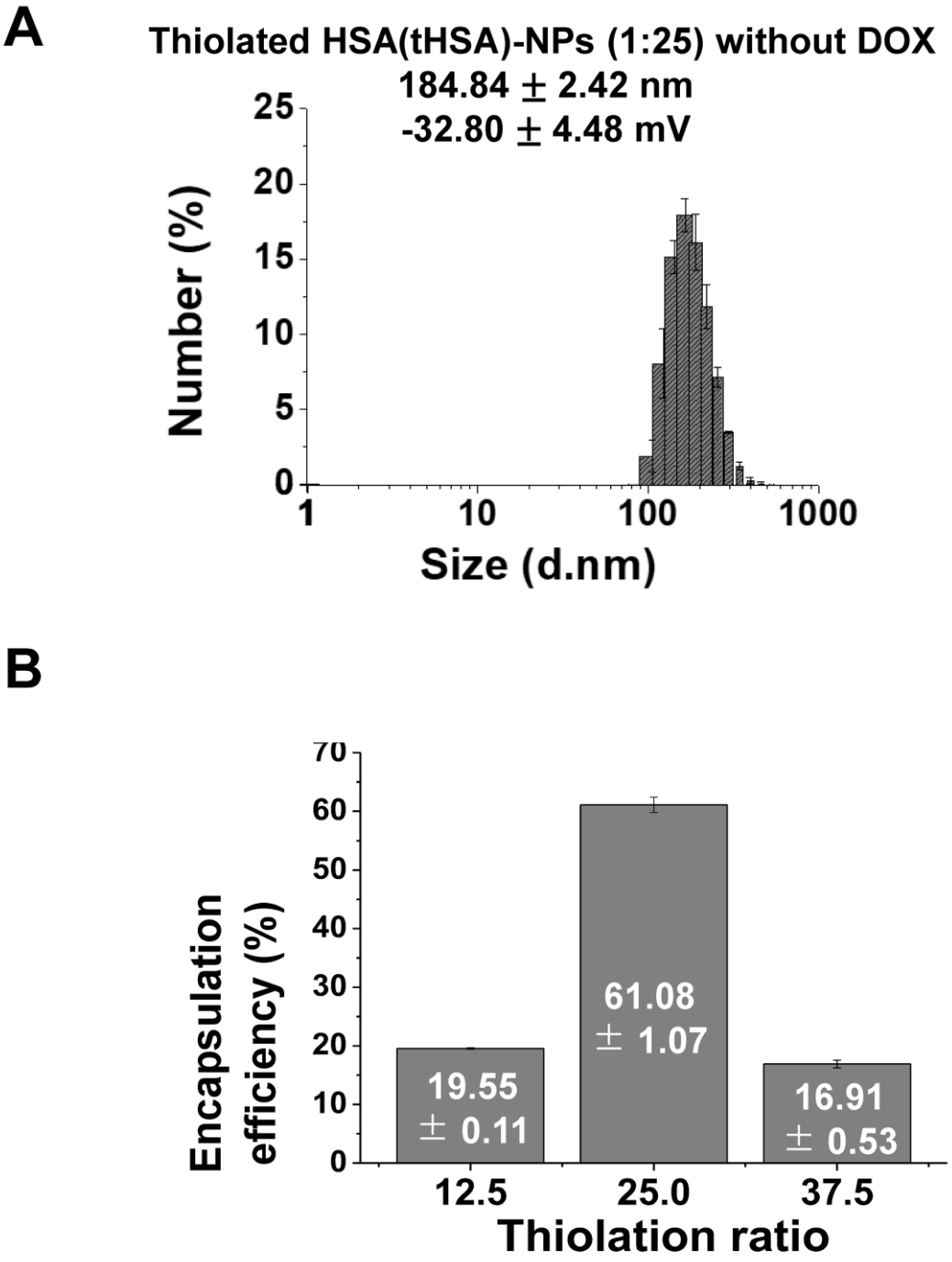

(A) Size of tHSA-NPs measured by Dynamic Light Scattering (DLS); (B) Encapsulation efficiency corresponding to thiolation ratio (2-IT mole ratio per albumin molecule)

Supplementary Figure S2

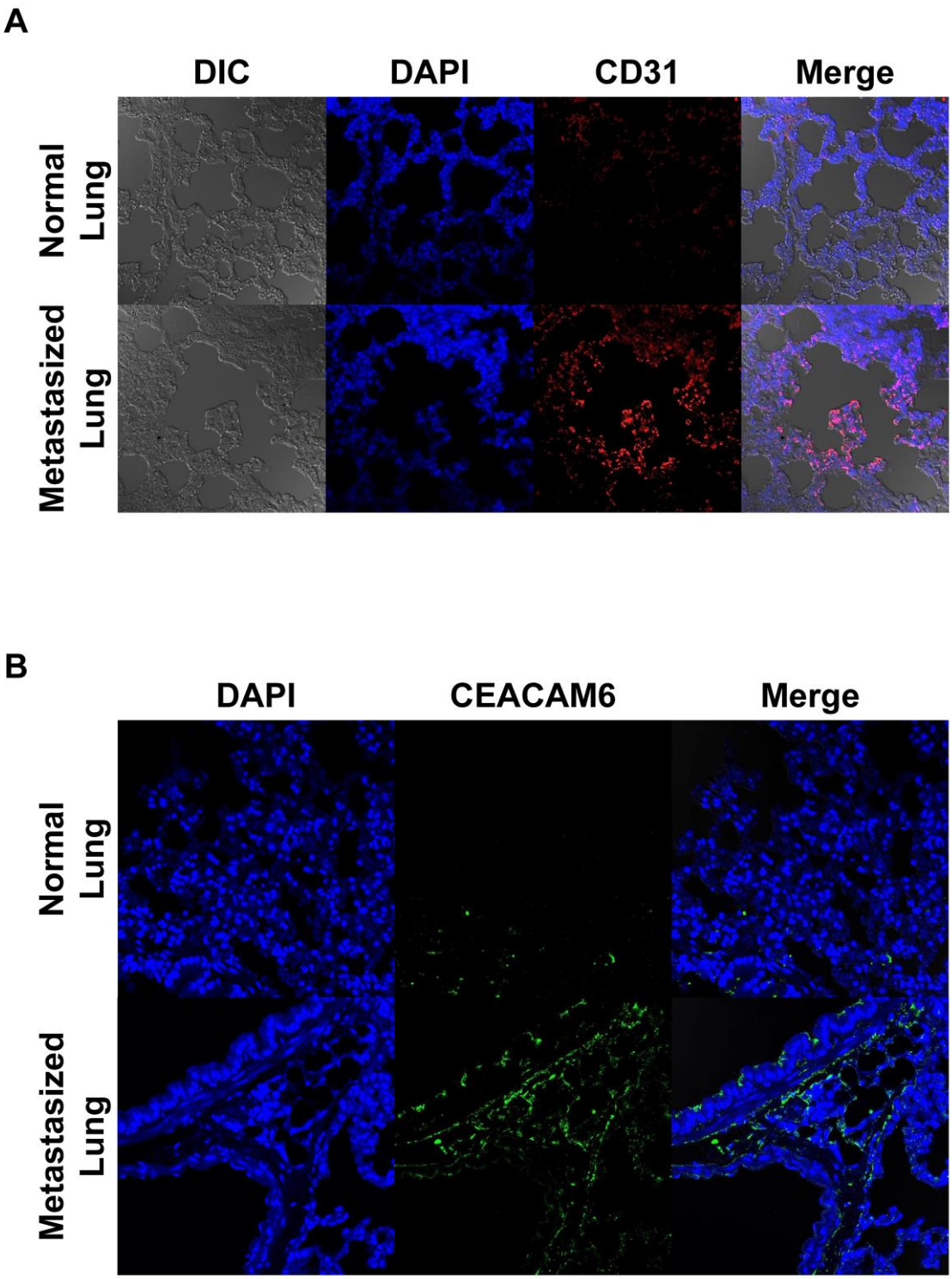

Immunohistochemistry images of normal and A549 AR-metastasized lung tissues. (A) Expressions of CD31 (neovascularization factor) and (B) CEACAM6 were higher in metastasized lung compared to normal lung.

Supplementary Figure S3

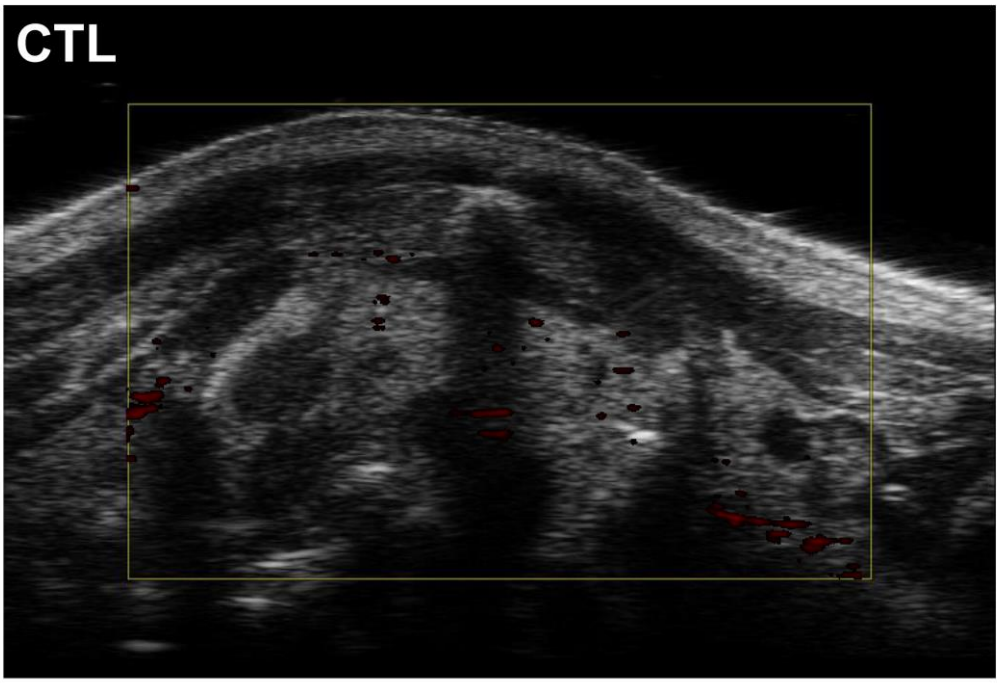

In vivo photoacoustic image of control (no injection) group using a Vevo LAZR Imaging System

Supplementary Figure S4

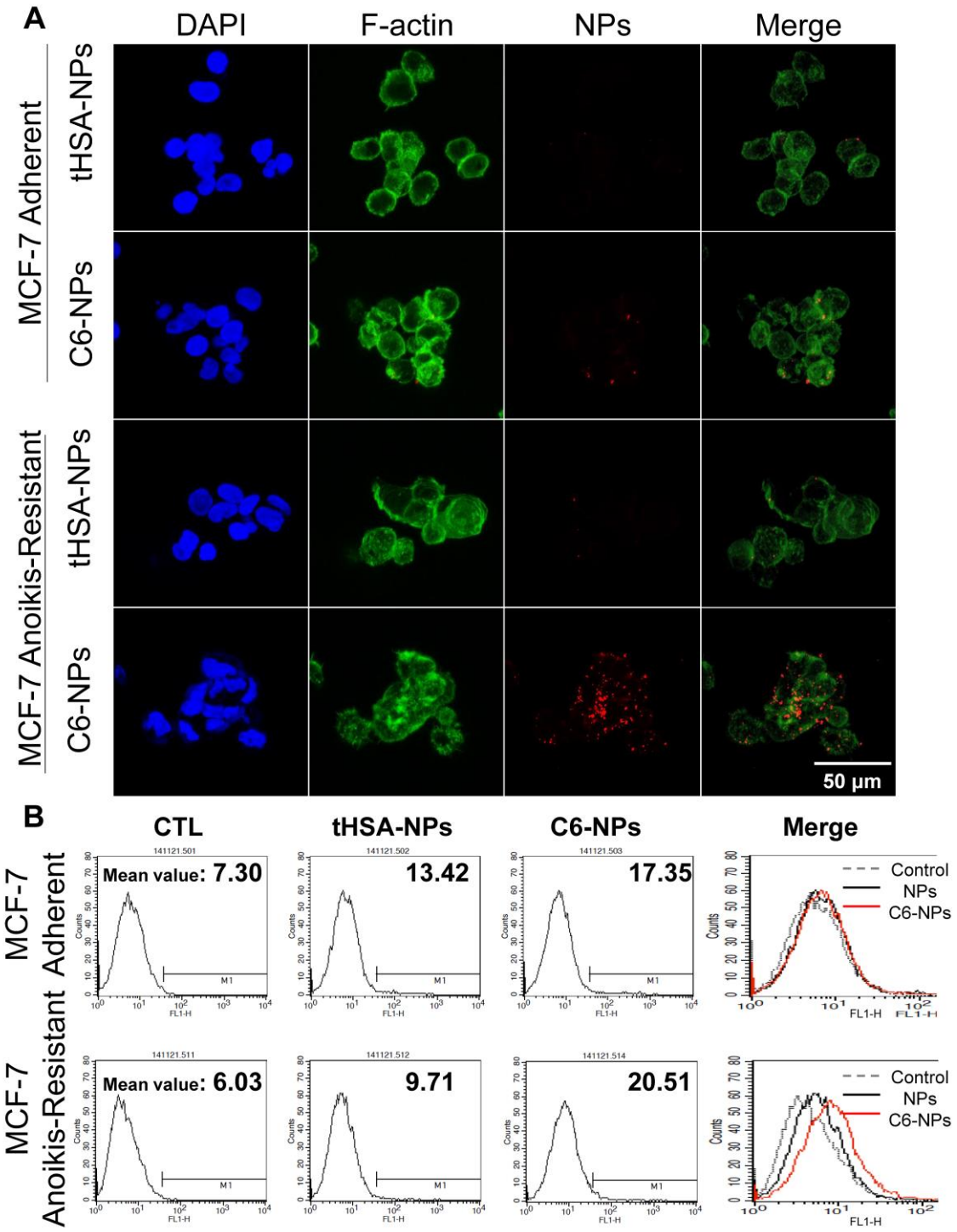

(A) Cellular targeting of CEACAM6-targeting tHSA-NPs (C6-tHSA-NPs) to MCF-7 adherent and MCF-7 AR cells under the shaking media condition for 30 min. Cell nucleus, F-actin and nanoparticles were shown as blue, green, and red, respectively. The rightmost column represents merged images of all. (B) Flow cytometry data for quantification of cellular targeting in the same condition.

Supplementary Figure S5

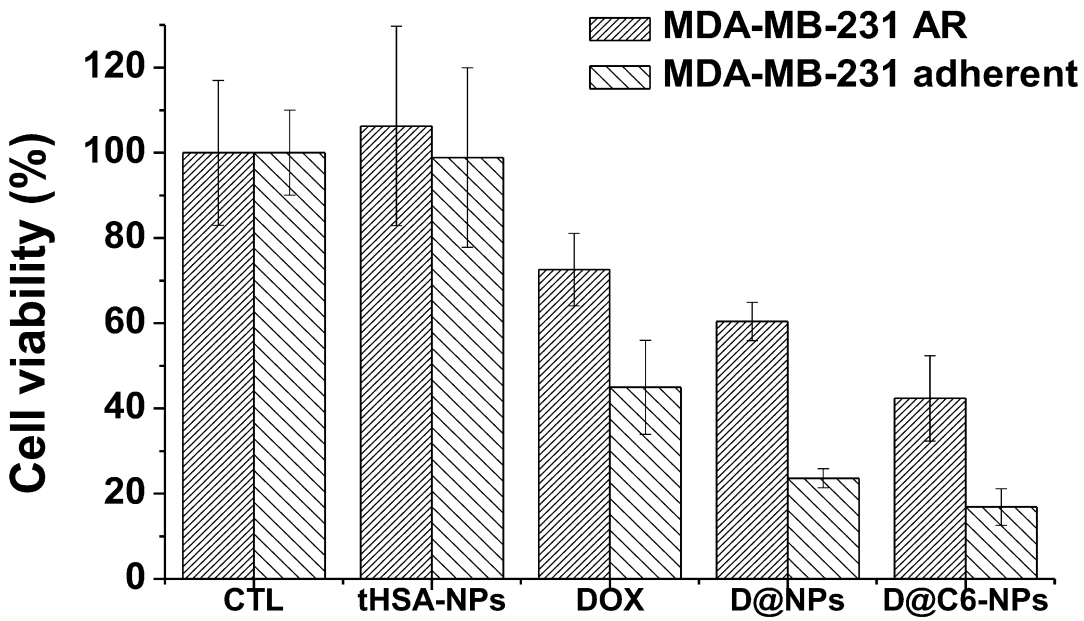

Cell viability assay with parental MDA-MB-231 adherent and MDA-MB-231 AR cells. Cells were treated at a concentration corresponding to 100 nM DOX for 6 h and further cultured up to 72 h in fresh medium. Bar with dense line and sparse line represent MDA-MB-231 adherent and MDA-MB-231 AR cells, respectively.

Supplementary Figure S6

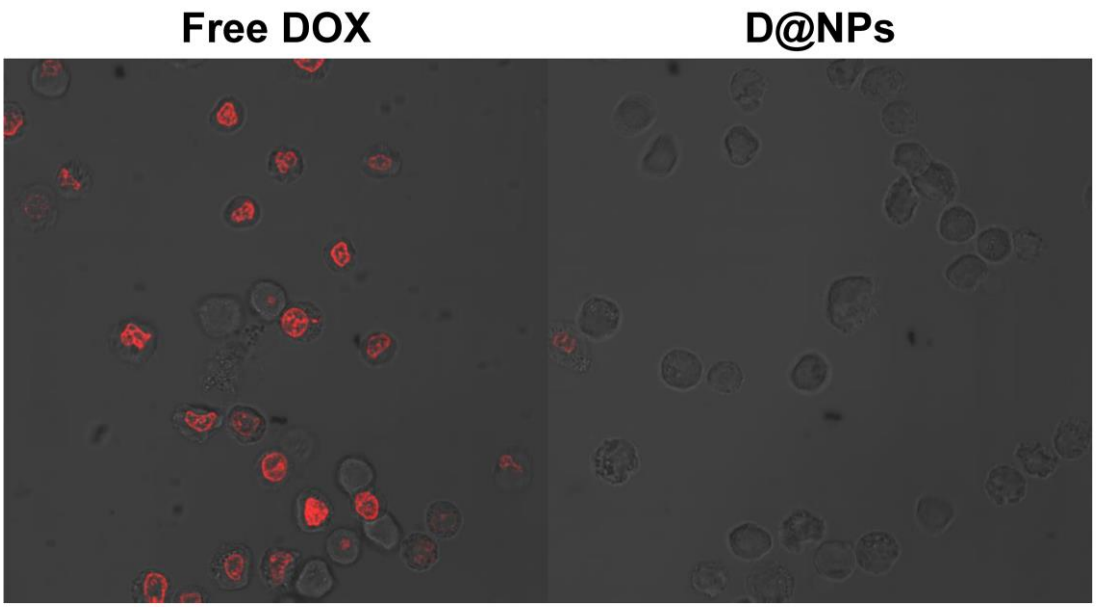

DOX uptake images to A549 AR cell nucleus under the shaking condition mimicking *in vivo* blood flow. Diffusion of free DOX was more efficient than DOX delivered by D-tHSA-NPs in this condition. Cells were treated at a concentration corresponding to 10 μM DOX for 1 h.

Supplementary Figure S7

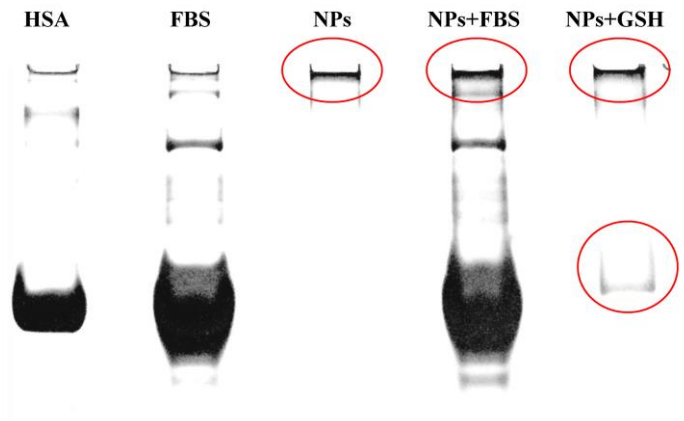

Serum stability and degradation by glutathione of tHSA-NPs. 50 (vol.%) FBS and glutathione was treated with concentration of 1.5 mg/ml to tHSA-NPs for 1 hour. Gel retardation assay was performed with SDS-PAGE and protein was stained with coomassie blue.

Supplementary Figure S8

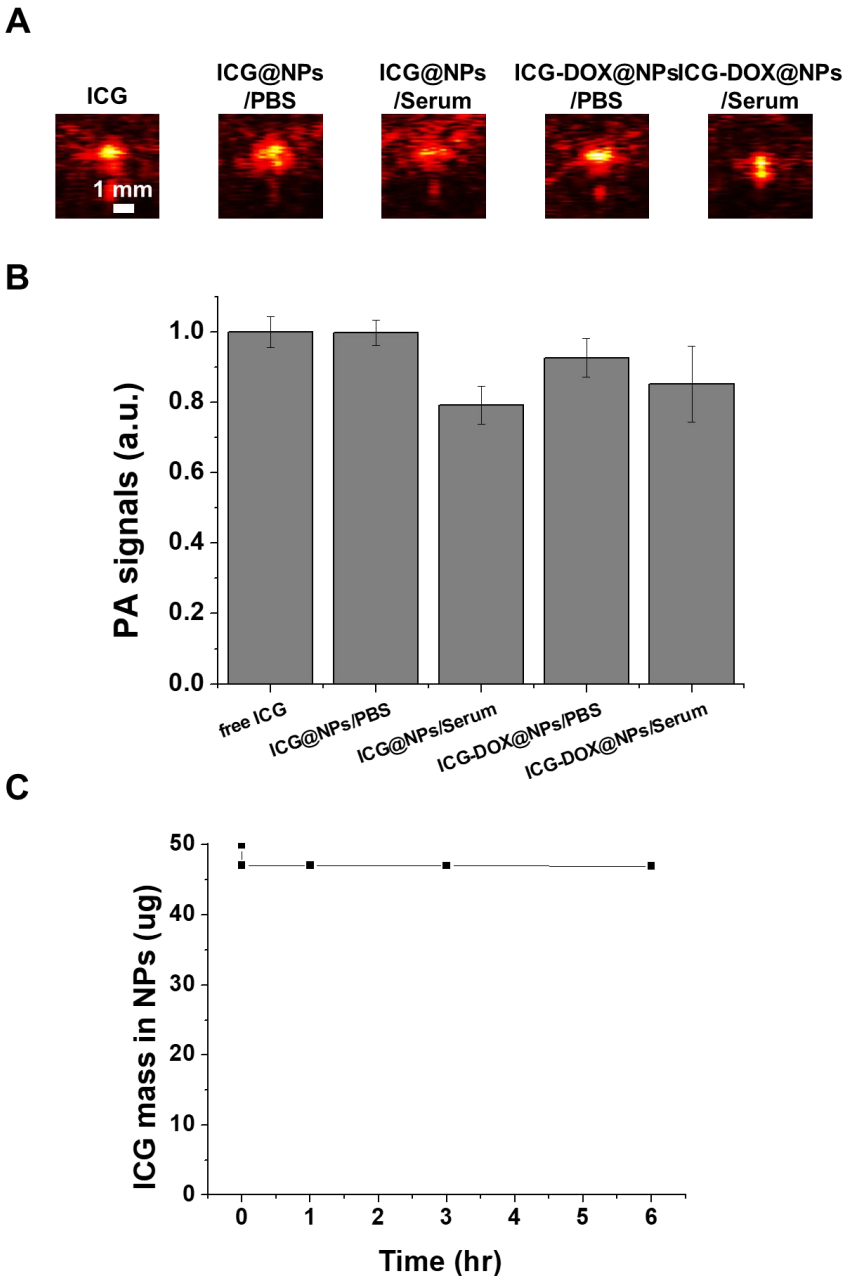

(A) Photoacoustic contrast ability and (B) its quantification graph of the ICG-containing nanoparticles (I@NPs and I+D@NPs) dispersed in PBS and 50% FBS solution. The result shows that there are no significant changes of PA contrast ability after 24 hours in serum condition. (C) ICG mass in nanoparticles (I@NPs/PBS, 37 °C) over time.

Supplementary Figure S9

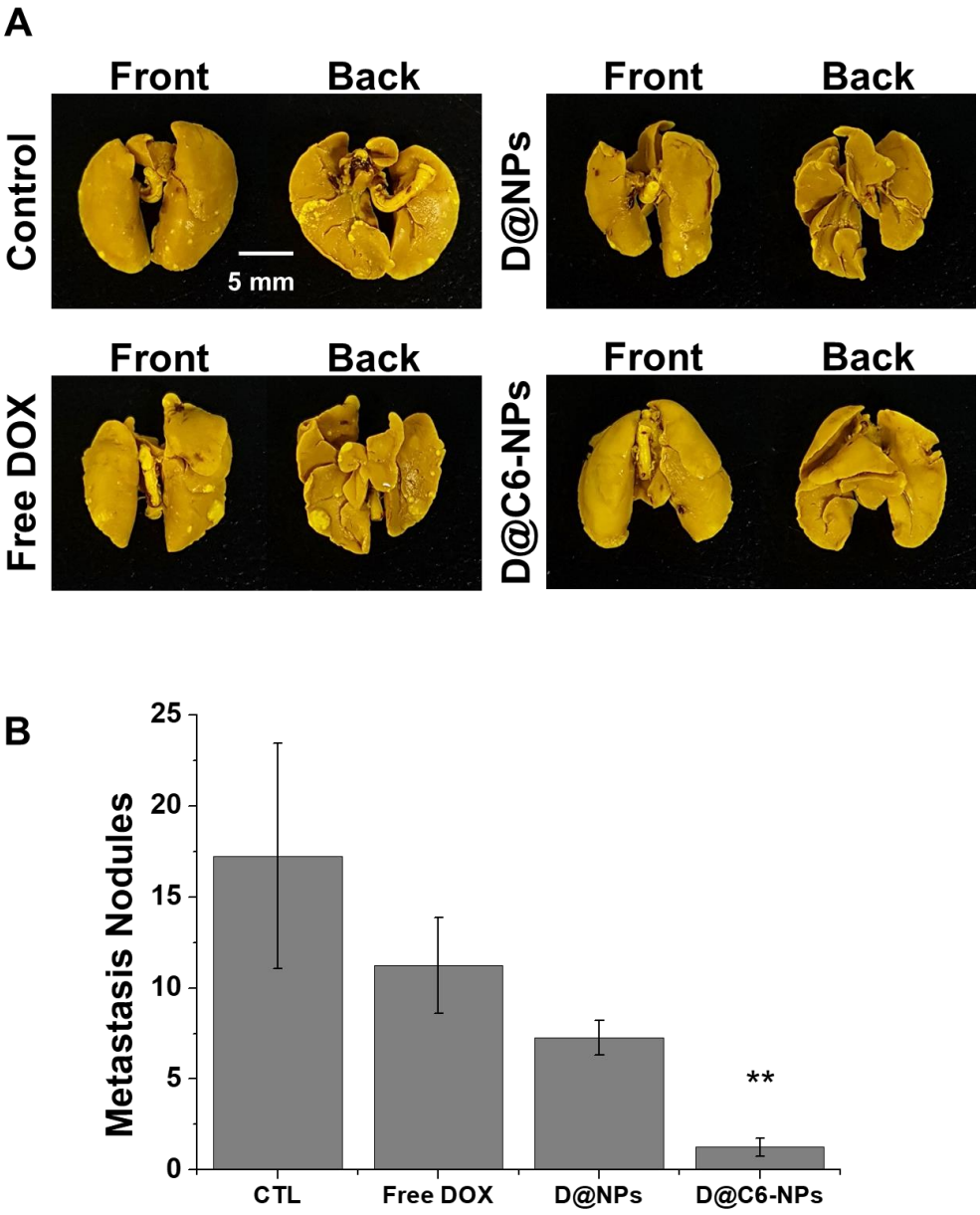

(A-B) *In vivo* tumor growth inhibition of D@C6-NPs and other groups. Three days after the intravenous injection of A549 AR cells, the first therapy was conducted. After 3 days, the second therapy was performed. Metastatic nodules in BALB/c nude mouse lungs were photographed and the number of metastatic nodules was quantified. D@C6-NPs group displayed statistical significance (ANOVA, $p<0.01$).

Supplementary Figure S10

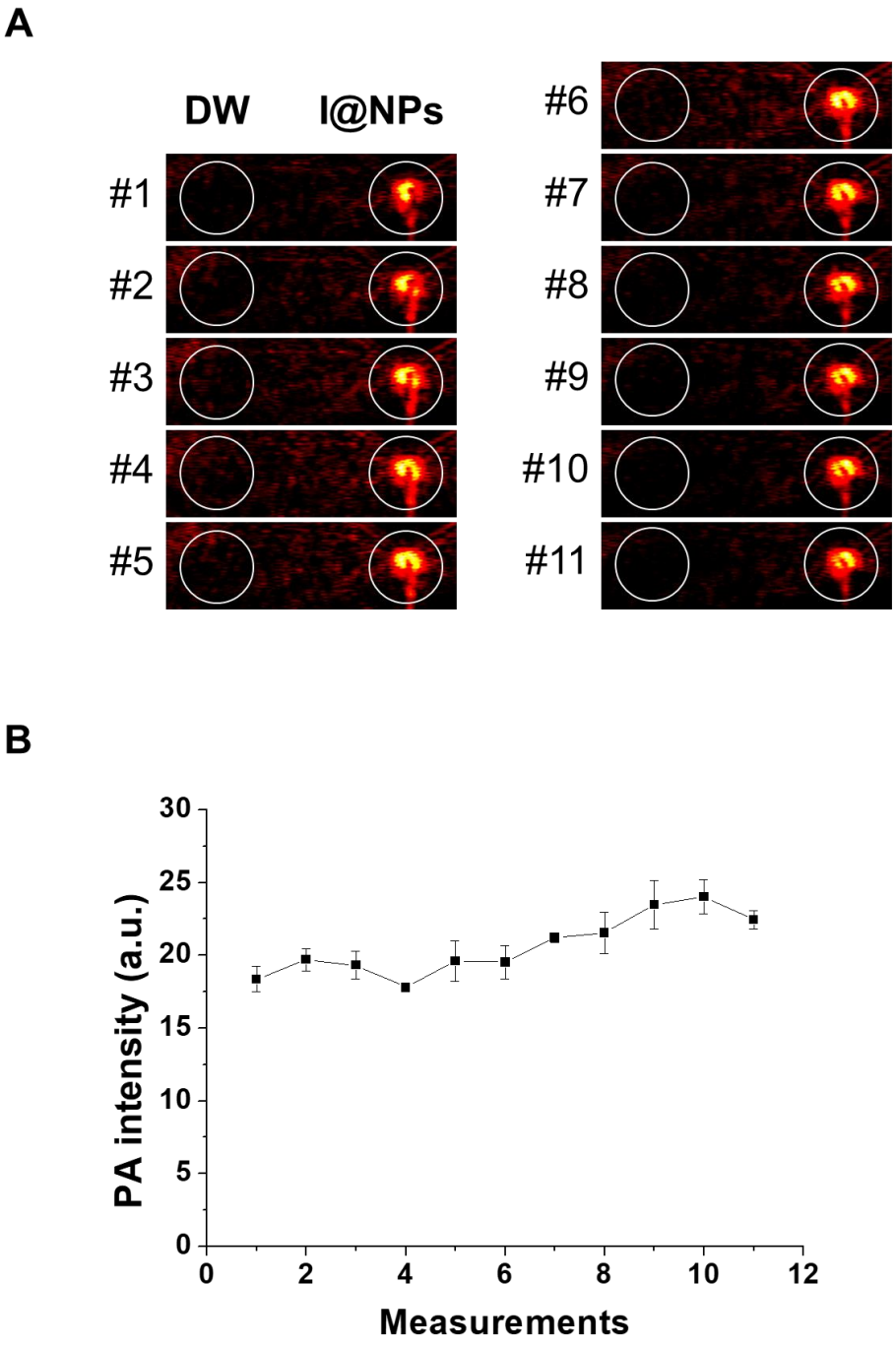

(A-B) Stability of photoacoustic contrast ability of I@NPs for multiple laser irradiation. The result shows that there is no reduction in the photoacoustic signal even after multiple laser exposures.

Supplementary Figure S11

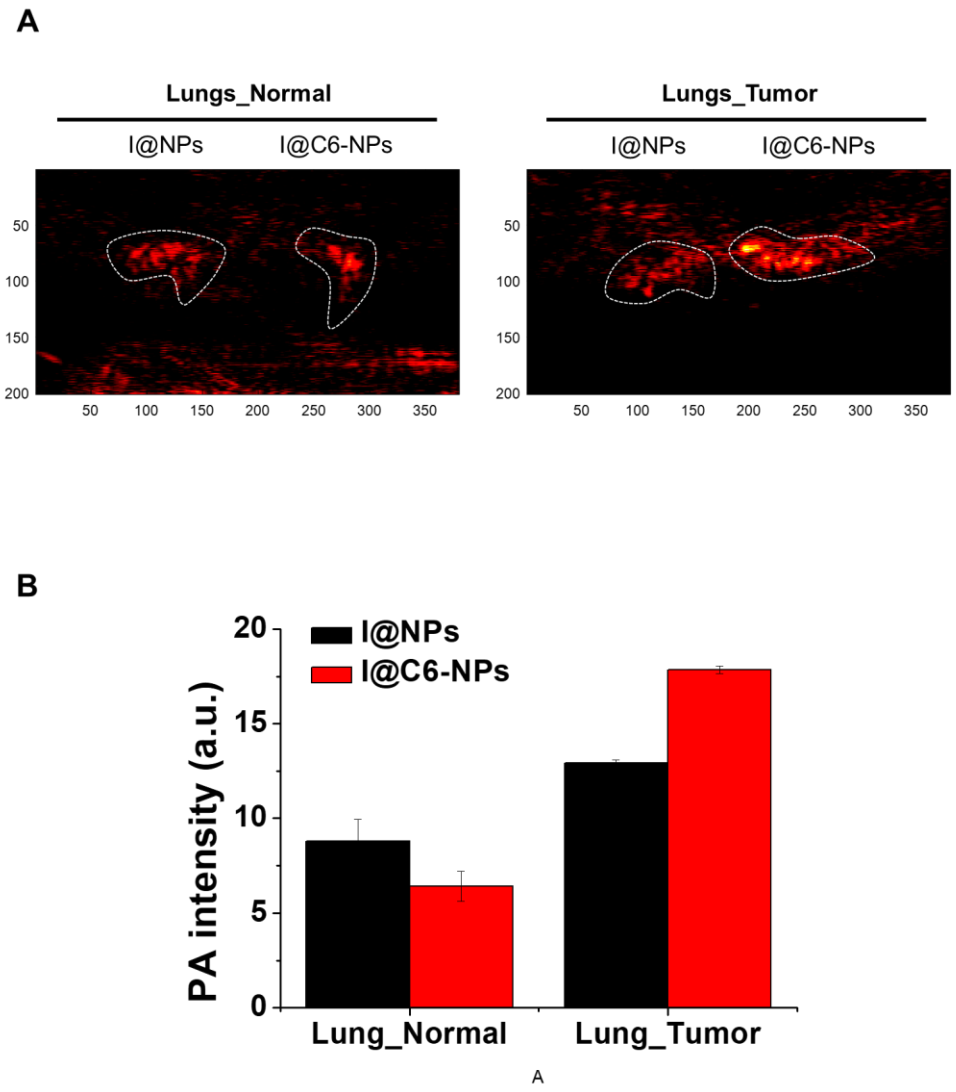

(A-B) *Ex vivo* PA images of both I@NPs and I@C6-NPs from normal and metastasized lungs and its quantification data. L7_4 transducer was used to obtain *ex vivo* photoacoustic images. Lungs were extracted 24 h after the injection of both I@NPs and I@C6-NPs.